

PHOTOMASK

BACUS—The international technical group of SPIE dedicated to the advancement of photomask technology.

EUV Lithography - Invited Paper

High-NA EUV Lithography Exposure Tool: Advantages and Program Progress

Jan van Schoot, Sjoerd Lok, Eelco van Setten, Ruben Maas, Kars Troost, Rudy Peeters, Jo Finders, Judon Stoeldraijer, and Jos Benschop, ASML, De Run 6501, 5504 DR Veldhoven, Netherlands

Paul Graepner, Peter Kuerz, and Winfried Kaiser, Carl Zeiss SMT GmbH, Rudolf-Eber-Straße 2, 73447 Oberkochen, Germany

ABSTRACT

While EUV systems equipped with a 0.33 Numerical Aperture (NA) lens are entering high volume manufacturing, ASML and ZEISS are in parallel ramping up their activities on an EUV exposure tool with an NA of 0.55.

The intent of this high-NA scanner, targeting a resolution of 8nm, is to extend Moore's law throughout the next decade. The high-NA optical system, together with the developments in mask and resist, provides an increased contrast, key to control stochastic contributions to EPE and the rate of printing defects.

A novel lens design, capable of providing the required NA, has been identified; this lens will be paired with new, faster stages and more accurate sensors enabling the tight focus and overlay control needed for future process nodes. Impact on system architecture and proposed solutions are described in this paper.

In addition, we give a status update on the developments at ZEISS and ASML.

1. Introduction

Up to now, commercially available EUV step & scan systems offer an NA of 0.33^{[1][2]}, allowing 13 nm resolution for dense lines at single expose. Multiple patterning or a larger NA is required in order to facilitate further shrink. Figure 1 shows that both scenarios are considered in the long term ASML EUV product roadmap.

Stochastics control is based on three pillars: aerial image contrast, resist and dose. The first is described in section 2 as a key benefit of high-NA, where a contrast roadmap is also proposed. Improved contrast will strongly reduce the defect printability rate. We will elaborate on the involved mechanisms. For this, a stochastic resist simulator has been developed. Where traditionally Line Width Roughness (LWR) and Local CDU (LCDU) are used as a measure to predict print fidelity, we will show that the photons in the centre of the printed contact hole play an important role, rather independent from the LCDU.

In order to reduce the angular range at the mask and the shadowing effects, a fully new anamorphic system needed to be developed^[3]. This novel system architecture is now designed and being implemented, and its impact is described in section 3.

Based on all knowledge of the optics manufacturing process, the imaging properties of the high-NA system can be predicted. These are described in section 4. In addition, photoresist progress is discussed in section 5, as key for improving LWR (line width roughness) performance.

In order to industrialize the high-NA system, manufacturing equipment is installed all over the world. At Zeiss, optics production has started. At ASML, the first parts for the mask and wafer stages are being assembled. A status update is given in section 6.

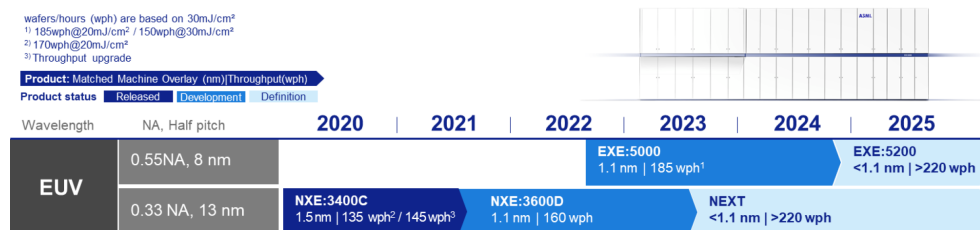


Figure 1. The current ASML EUV product roadmap.

BACUS

N • E • W • S

MAY 2021
VOLUME 37, ISSUE 5

TAKE A LOOK
INSIDE:

INDUSTRY BRIEFS
—see page 12

CALENDAR
For a list of meetings
—see page 13

SPIE.

EDITORIAL

What good is it all doing? A quick look back and then forward again

Stephen Renwick, Nikon Research Corp. of America

Back in school, were you thinking that you might grow up to go out there and save the world? Or at least, did you vow to make it a better place? Sure you did. With that science or engineering degree firmly in hand, you would work on the cure for cancer, or limitless energy from clean fusion power, or the chemical breakthrough that would triple our grain production for a hungry world. A small Nobel or similar would of course be a nice token of appreciation.

Perhaps your professional career wasn't quite so glamorous as planned, but we can take credit that our own particular industry is responsible for the data-handling and worldwide communication that we all take for granted. Grandparents used to receive postcards from their grandchildren — now they see the kids on the phone. Maskmakers and lithographers didn't invent the COVID vaccine, but we can bet that said invention would have been a lot more difficult without the computing power that our industry helped to make possible.

Would you like another example? Go stand outside next to a really busy street. Take a deep breath. Did you cough, or smell a cloud of unburnt hydrocarbons? Probably not.

Automobiles touch all our lives. Consider a few not-especially-random examples. A 1973 VW Bug was the premier economy car of its day. Mine sported about fifty horsepower, accelerated as if the engine were tied to the bumper instead of powering the wheels, and got all of about 25 miles to the gallon on a good day. Fourteen years later, a 1987 Saab was bigger, considerably more comfortable, had just over a hundred horsepower, and still got about 25 miles to the gallon. Another fourteen years later, a 2001 BMW (yes, there's a trend here) was even bigger, had almost two hundred horsepower, and still returned 25 miles to the gallon. Meanwhile, the pollution coming out of the tailpipe, unburnt hydrocarbons and nitrogen oxides, dropped by a factor of ten, in response to Federal regulations.

What does that have to do with photomasks? The enabling technology for that revolution in efficiency was electronic fuel injection and engine control. On the dear old Bug, the only electronics was in the radio. The Saab had a mechanical continuous fuel-injection system with electronic feedback control. The BMW had fully electronically-controlled fuel injection with a preprogrammed "map" as well as sensors for temperature, exhaust oxygen content, and fuel-air mixture, as well as electronic control of the intake and exhaust valves. Our colleagues in automotive engineering are smart folks, and made excellent use of the electronic revolution that our industry created.

That hasn't ended. As I write this, automobile companies in the US are cutting production due to a global chip shortage. Autonomous vehicles will need on-board artificial intelligence as well as fast communication. Software manages the charging and discharging of electric cars, lengthening their range and battery life.

To continue making the world a better place, our industry must supply not only leading-edge memory and logic chips, using EUV and its associated techniques, but also more and more larger-scale analog and digital electronics for machine control and artificial intelligence, challenging us to make better use of legacy technology. The Photomask Technology and co-located EUV conferences this fall will continue to explore these challenges. It's a great time to be here.



N • E • W • S

BACUS News is published monthly by SPIE for BACUS, the international technical group of SPIE dedicated to the advancement of photomask technology.

Managing Editor/Graphics Linda DeLano
SPIE Sales Representative, Exhibitions, and Sponsorships
Melissa Valum
BACUS Technical Group Manager Tim Lamkins

■ 2021 BACUS Steering Committee ■

President

Emily E. Gallagher, imec.

Vice-President

Kent Nakagawa, Toppan Photomasks, Inc.

Secretary

Jed Rankin, GLOBALFOUNDERIES Inc.

Newsletter Editor

Artur Balasinski, Cypress Semiconductor Corp.

2021 Photomask + Technology Conference Chairs

Stephen P. Renwick, Nikon Research Corp. of America
Bryan S. Kasprovicz, HOYA

Members at Large

Frank E. Abboud, Intel Corp.
Uwe F. W. Behringer, UBC Microelectronics
Peter D. Buck, Mentor Graphics Corp.
Brian Cha, Samsung Electronics Co., Ltd.
Aki Fujimura, DS2, Inc.
Jon Haines, Micron Technology Inc.
Naoya Hayashi, Dai Nippon Printing Co., Ltd.
Bryan S. Kasprovicz, HOYA
Romain J. Lallement, IBM Research
Patrick M. Martin, Applied Materials, Inc.
Jan Hendrik Peters, bmbg consult
Douglas J. Resnick, Canon Nanotechnologies, Inc.
Thomas Scheruebl, Carl Zeiss SMT GmbH
Thomas Struck, Infineon Technologies AG
Bala Thumma, Synopsys, Inc.
Anthony Vacca, Automated Visual Inspection
Vidya Vaenkatesan, ASML Netherlands BV
Andy Wall, HOYA
Michael Watt, Shin-Etsu MicroSi Inc.
Larry Zurbrick, Keysight Technologies, Inc.

SPIE.

P.O. Box 10, Bellingham, WA 98227-0010 USA
Tel: +1 360 676 3290
Fax: +1 360 647 1445
SPIE.org
help@spie.org

©2021

All rights reserved.

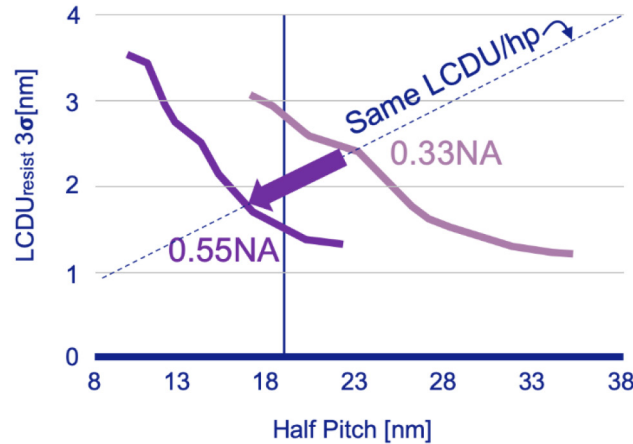


Figure 2. High-NA contrast reduces Local CDU for dense contact holes. All simulations are carried out using the same dose of $20\text{mJ}/\text{cm}^2$. See text for more explanation.

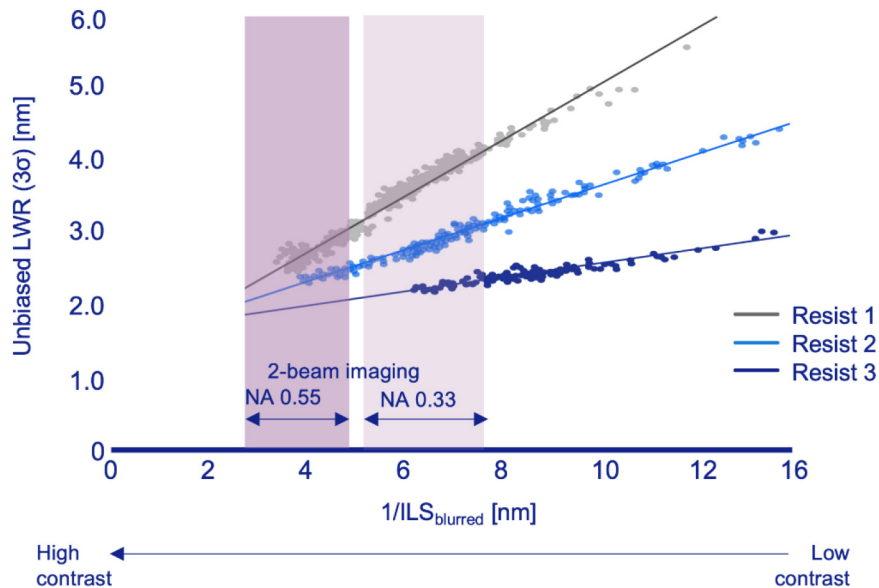


Figure 3. LWR scaling with $1/\text{ILS}$ extends to High-NA obtainable ILS values. The high contrast is made by printing large pitches on a 0.33NA EUV scanner. The three lines depict the behavior of three different resists.^[6]

2. The Key Advantage of High-NA: Improving Contrast

The novel EUV system features 0.55 NA projection optics, in contrast to the 0.33NA of the preceding generation. One of the main consequences of the increased NA is that the aerial image contrast at wafer will be larger when printing the same structures. The improved contrast will help print higher resolution features and reduce the impact of photon shot noise on pattern variability and defectivity.

The role of contrast in pattern variability and defectivity will be described in section 2.1 and 2.2. Section 2.3 will describe briefly the impact of advance masks to further increase the aerial image contrast.

2.1 High contrast leads to an improved LWR / LCDU

The predicted LWR is given in equation 1^{[4][5]}

$$\text{LWR}_{3\sigma, \text{ unb}} = k_4 \cdot e^{\left(\frac{\sqrt{2}\pi\sigma}{p}\right)^2} \cdot \sqrt{\frac{h\nu}{D_{\text{thr}}}} \cdot \frac{1}{\text{ILS}}$$

Whereby:

- σ = resist blur [nm]
- k_4 = contains Quantum Efficiency and absorption
- D_{thr} = dose to clear [mJ/cm^2]
- ILS = image log slope [$1/\text{nm}$]
- p = pitch [nm]

In general, a larger NA results in higher ILS, and in turn a lower LWR. This is shown in figure 2: at the same pitch, the LWR or LCDU is significantly smaller at 0.55NA compared to 0.33NA. Note that at resolutions below $\sim 16\text{nm}$, the dense contact hole arrays cannot be resolved using the 0.33NA system, leaving higher NA as the only option for single exposure.

Despite the fact that LCDU and LWR are important measures for stochastic performance, LCDU relative to the target CD is actually the relevant metric. This is depicted by the diagonal dashed line in figure 2: all points on this line have the same LCDU/CD ratio. The arrow depicts the resolution advantage (maintaining constant relative performance) of high-NA compared to 0.33NA systems.

One notable assumption is that photoresists are capable of translating the 0.55NA improved contrast into reduced LWR or LCDU. To verify this, an experiment was carried out on a 0.33 NA system where the aerial image contrast was increased deliberately for relaxed resolutions. Because of the large pitches (50.5 and 88.0 nm LS) more orders are available, resulting in higher contrast. The contrast was modified from this optimal point by varying focus and dose. Figure 3 shows that the measured LWR clearly correlates with $1/\text{ILS}$ as expected from equation 1, for the three different resists that were used in the experiment.

During the experiment the following conditions were used:

- Dense Lines and Spaces, pitches 50.5nm and 88.0 nm

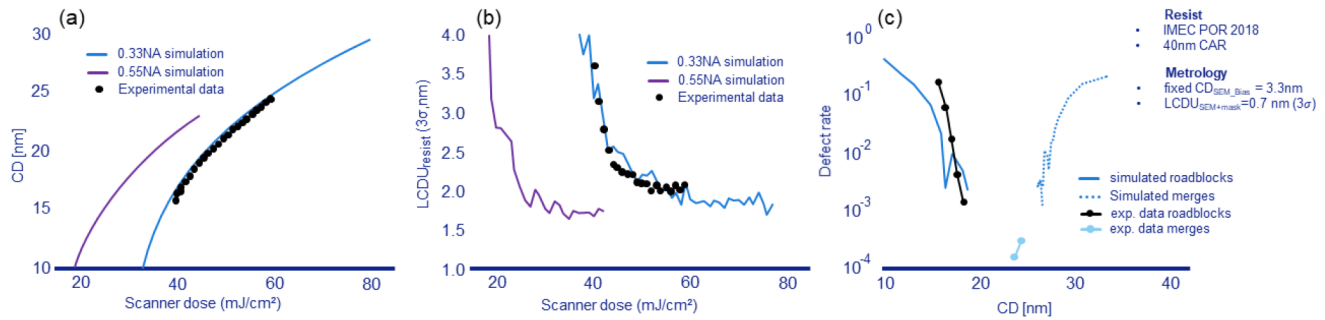


Figure 4. Stochastic resist simulations calibrated to experimental data of regular P40 contact holes printed with a CAR used as process of record at imec in 2018. Calibration included matching CD (a) and LCDU (b) for varying scanner dose. The failure rate was also simulated (c).

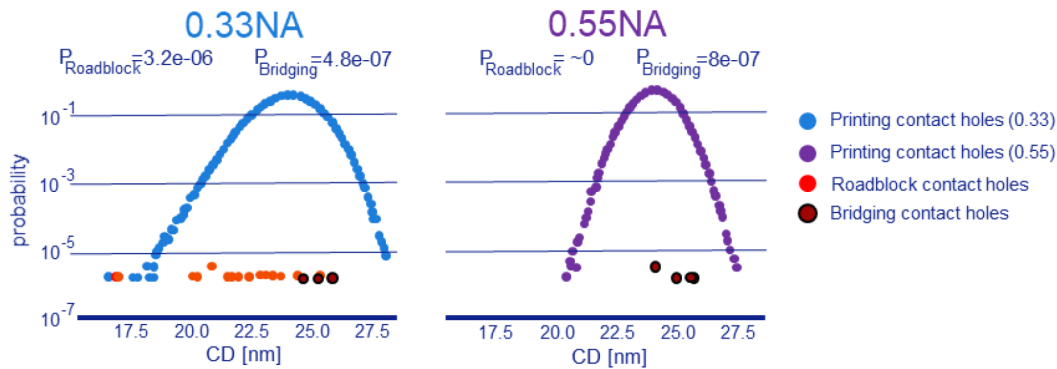


Figure 5. CD distributions for 0.33NA and 0.55NA around a target CD of 24 nm. Apart from printing contact holes that print properly (indicated by their Critical Dimension), also roadblock and bridging failures are indicated.

- Optimized illumination pupil settings to achieve highest contrast
- Contrast is reduced by varying dose & focus
- $ILS_{blurred}$ is derived from the experimental normalized dose sensitivity
- The metrology contribution to the LWR is removed (so called unbiased LWR) by subtracting the noise floor from the power spectral density (PSD) of the measured resist contours.^[7]

Based on the results as shown in figure 3, we can make the following conclusions:

- LWR continues to scale towards $1/ILS_{blurred}$ down to ~3nm.
- All resists show the same trend, differences are due to specific resist properties.
- Extrapolation towards $1/ILS \rightarrow 0$ does not yield a LWR of 0, it is expected that the LWR floor is caused by chemical variability of the resist, such as local variation of the PAG and/or quencher density.

2.2 High Contrast leads to a reduced defect rate

Photon shot noise and local inhomogeneities of the resist cause pattern variability, as quantified by LCDU and LWR. In extreme cases these sources of noise can also lead to patterning defects, such as missing/merging failures for contact holes, and bridges/breaks for line/spaces. For some advanced patterning applications, it can be found that these stochastic defects limit device yield more than the CD or LCDU/LWR based process windows. To compare the patterning performance of 0.55NA with 0.33NA we have used stochastic resist simulations for a fixed use-case of regular pitch 40 nm contact holes to determine expected stochastic failure rates^[8].

The CAR model used in the stochastic simulations is calibrated using CD and LCDU data through dose. As can be seen in Figure 4 both the simulated CD and LCDU match the experimental values well. For a target CD of 20 nm the dose to size was 45 mJ/cm² for 0.33NA and 33 mJ/cm² for 0.55NA. Note that the same resist model was used for both conditions, which means that the resist dose to clear is fixed. The dose to size is lower for the 0.55NA use-case, because the higher NA transmits more light from the mask to the wafer as higher diffraction orders are captured. At this target CD the LCDU goes from about 2.4 nm (3σ) for 0.33NA to 1.7 nm (3σ) for 0.55NA because of the higher image log slope. The predicted defect rate (Fig. 4(c)) for 0.33NA matches experimental

values within an order of magnitude, despite the fact that this data was not included in the model calibration.

Stochastic defectivity is evaluated for a target CD of 24 nm. Figure 5 shows the CD distribution for the 0.33NA and 0.55NA use-case. This figure shows that the CD distribution for 0.55NA is much narrower as compared to the 0.33NA distribution. Reason for this is the higher image log slope. Furthermore, at 0.33NA we encountered both roadblock and bridging failures, indicating there is no defect free process window for this resist. For 0.55NA, we still observe a few bridging failures, but no roadblock failures at all. Because we are in this case no longer suffering from roadblock failures, the target CD can be chosen smaller to reduce the bridging failure rate accordingly. This is an encouraging result which demonstrates the effectiveness of improved optical contrast in reducing defectivity.

The reason we no longer observe any roadblock failures for the 0.55NA use-case is that the number of photons in the center of the contact hole is much higher. This is true even though the dose to size for the 0.55NA use-case is lower, because the higher NA allows the light to be focused more tightly. Figure 6 shows a quantitative comparison between the aerial image intensity of the 0.33NA and 0.55NA use-case, where the intensity has been normalized to the dose to size. The gray regions ① indicate the aerial image contrast close to the edge of the feature, relevant for the LCDU. The colored center regions ② are relevant for determining the probability of roadblock defects. As can be seen, the center region receives on average two times more photons for 0.55NA than for 0.33NA. Such a relative increase in local dose can have a significant influence on the failure rate, as also observed in experimental data^{[9][10]}.

So far, we looked at the differences when printing the same pattern with Single Exposure on both 0.33NA and 0.55NA systems. As expected, a clear advantage of the higher NA is observed. The next step is to compare the expected behavior of a pattern that is below the Single Exposure capabilities of the 0.33NA tool, so Double Exposure is needed for 0.33NA, Single Exposure is enough for 0.55NA. A dense regular CH pattern printed twice on a 0.33NA tools yields a 28nm pitch staggered CH pattern. This same pattern can be printed in one exposure with a 0.55NA lens. The aerial images of are shown in figure 7. Despite the smaller pitch on the 0.55NA system, the slope is 1.35x larger and the

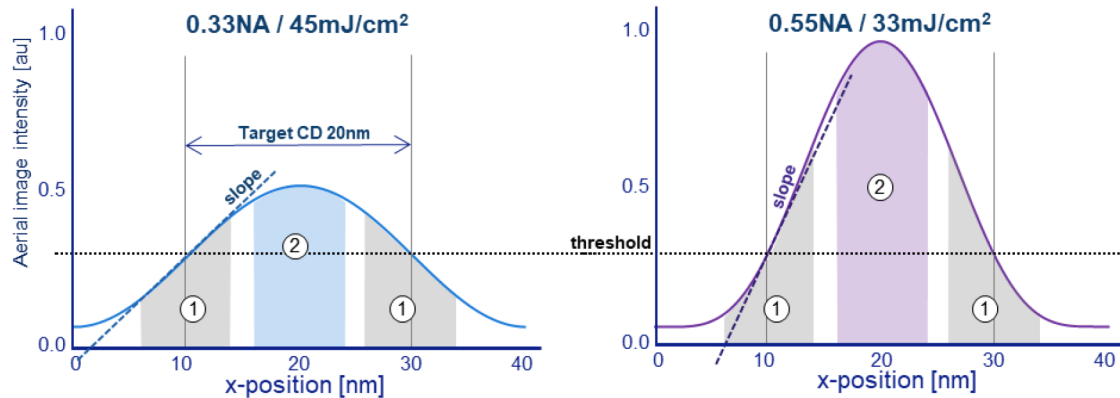


Figure 6. Normalized aerial image intensity for the two use cases. The 0.55NA use-case has significantly higher image log slope and center intensity, resulting in a lower LCDU and defect rates. The photons in the areas ① are merely determining the LCDU, where the photons in areas ② are enabling a clear developer path toward the bottom of the contact hole, and therefore determine the defect rate for roadblocks.

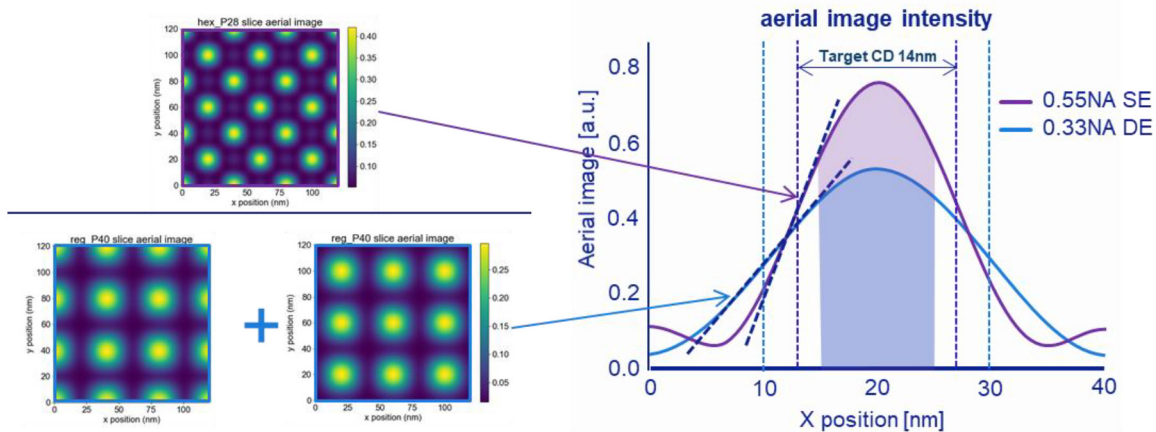


Figure 7. Normalized aerial image intensity for the two use cases. Now the 0.55NA system prints a 28nm staggered CH pattern in one go, where the 0.33NA systems needs a Double Exposure of a 40nm dense CH pattern to arrive at the same 28nm staggered pattern. The aerial image of 0.55NA case has a slope that is 1.35x larger and a number of photons in the centre of the hole that is 1.4x larger than the 0.33NA case. Based on this, a significant smaller amount of defects is expected on the Single Exposure 0.55NA pattern.

number of photons in the center of the hole is 1.4x larger than in case of the larger feature size as printed on the 0.33NA system. Based on this higher center intensity, a significantly lower defect rate is expected for the Single Exposure 0.55NA pattern.

2.3 Advanced mask as a means to further improve the aerial image contrast

As can be seen in figure 2, without additional measures contrast will go down with shrinking resolution, resulting in an increase of the stochastic contribution to the imaging and edge placement error. Therefore, it is key to keep the aerial image contrast high. One way to do this is by changing the mask configuration^[11]. In this context, increasing the absorption coefficient of the mask absorber or the introduction of a low-n, phase shifting absorber layer are well known methods^[12]. Additional improvements are expected to come from optimized photoresists (see section 5), better post processing and the increase of the exposure dose. Also new mask multi layer stacks are being proposed^[13]. Figure 8 shows the proposed contrast roadmap.

3. High-NA System Architecture

The architecture of the high-NA system has been extensively described in the past^{[14][15][16]} and its overall design is now finalized. We present here an overview of the main differences with respect to the 0.33NA system^[17] (figure 9).

Most important to mention here is that we had to introduce a so called anamorphic lens, with different x and y magnification of resp. 4x and 8x^[3]. As a result of the higher angles of the light on the optical

surfaces, a central obscuration was introduced^[18]. A consequence of this is that the traditional Zernike description of the wave front aberrations no longer hold due to non-orthogonality of the individual Zernikes. A better description is proposed by making use of so called Tatians^[19]. As a result of the required anamorphic projection, and the desire to maintain the existing 6" mask infrastructure, a half field is printed on the wafer. To ensure that the productivity of such a system is not reduced by this, the acceleration of the mask and wafer stages had to be increased by 4x and 2x, respectively. The resulting throughput graphs for both the 0.33NA NXE:3400C and the high-NA system are depicted in figure 10.

As mentioned earlier, one of the main design constraints for the high-NA system was to keep the existing mask infrastructure in place. The main aspects of mask projection on wafer are unchanged by moving from 0.33NA to 0.55NA, however there are some differences that are important to know. The overview of the new layout is depicted in figure 11, and the overview of changed and unchanged properties is given in table 1.

Keeping the mask, wafer and optics clean is very important, so these aspects are especially considered during the design of the system. The situation around the mask is designed such that eventual particles moving towards the mask will be pushed back by a gas flow. Simulations have been done to optimize the geometry and flows in such a way that maximum suppression is ensured. At the wafer the situation is different, since the main concern is the outgassing of the resist. In this context, the gasses can potentially enter the optics and damage the optical surfaces. This is solved by maintaining an overpressure inside the projection optics that ensures sufficient suppression of contaminants. Notably, the optional DGL membrane will not impact the overall vacuum architecture of the system. In figure 12, simulation results demonstrating the required sup-

Application timing	2020	2022	2024	2026	2028	2030
Lines and spaces [half pitch nm]	18	15	14	12	10	8
0.33NA NILS ¹	2.6	2.6	2.4			
0.55NA NILS ¹			2.8	2.7	2.6	
Staggered contact holes [half pitch nm]	22	21	20	18	17	16
0.33NA NILS ¹	4.0	3.9	3.4	3.3		
0.55NA NILS ¹				4.4	3.7	3.4
	TaBN absorber		Low-n absorber			

Figure 8. Proposed roadmap to maintain the image contrast for future nodes, using high-NA and advanced mask absorbers.

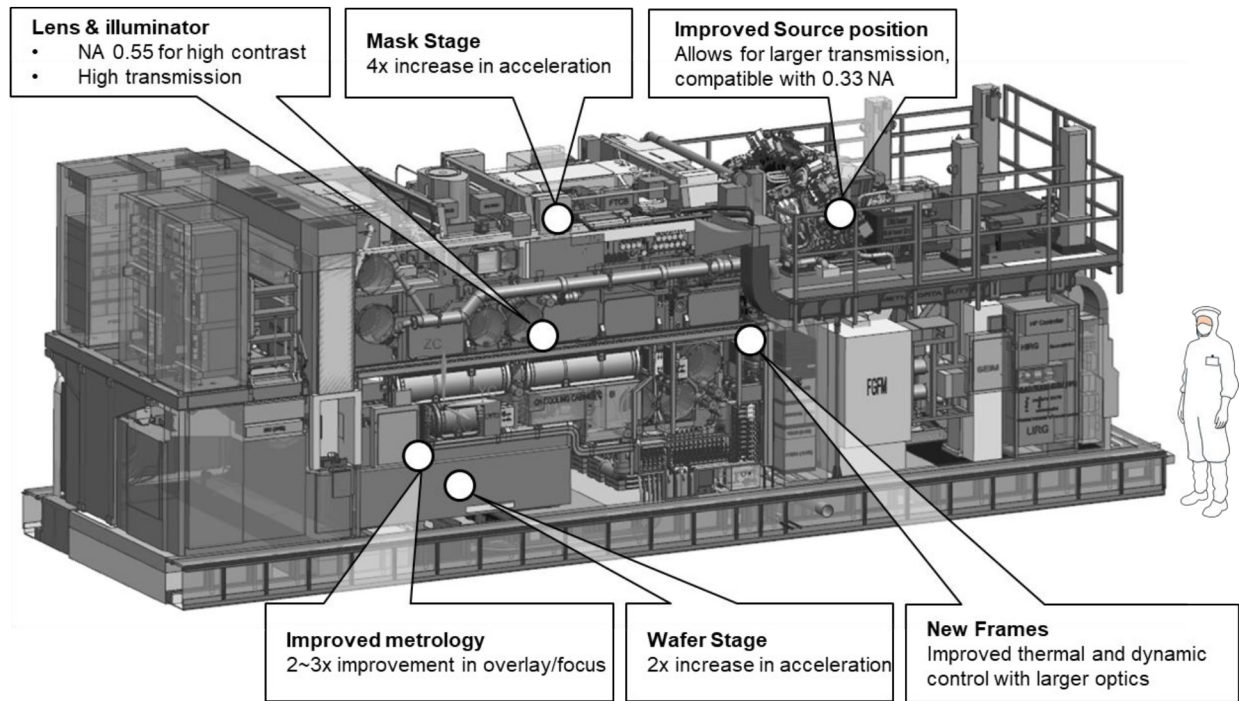


Figure 9. High-NA system architecture and highlight of the main differences with respect to the 0.33NA system.

pression are shown. Also a test setup for the experimental validation of the DLG suppression is currently being installed.

Another important change compared to the 0.33NA EUV system is the mask stage. Since the stage needs to operate at larger acceleration, the whole design has been reduced in weight significantly. This was done by, for instance, moving the cable slabs inside the vacuum^[20]. However, at these large accelerations the cable slabs are likely to release particles, which need to be suppressed in order to avoid mask contamination. Simulations have been carried out to optimize a shield that suppresses these particles. Moreover, experimental validation on witness sample showed one Teflon particle after 46 h of operation. Note that the particle shield is just a first layer of protection, and a second mechanical shielding will suppress these particles even further, see figure 13.

4. Expected Imaging Performance

In order to evaluate the expected imaging performance, a number of use cases have been defined. For each use case the pitches and pupil shape are defined. Importantly, the predictions of the performance are done based on the actual illuminator and source design, including the

aberrations and design tolerances. The overview of all cases (figure 14) shows that the expected outcome is well below the 10% target of CD error.

5. EUV Photoresist

One of the important boundary conditions for successful continuation of EUV in high volume manufacturing into the next nodes is the availability of good photoresists. For this we evaluate the progress of the different photoresists together with partners like IMEC, PSI and CXRO. In the overview below, the z-parameter is used as a metric for the resist quality^[14].

$$Z\text{-factor} = \text{Res}^3 \cdot \text{LWR}^2 \cdot \text{Dose}$$

Note that contrast is not a term in Z-factor equation, although earlier it was demonstrated that it is of impact on the LWR or LCDU of the printed structures. For this reason, the comparison is only valid at equal contrast. To also include the effect of contrast the novel k_4 paradigm has been introduced^[4].

Up to now, all our resist evaluations have been reported for 16nm lines and spaces (LS)^[17], where a continuous improvement in the resist quality can be observed. Recently we have started using more aggressive

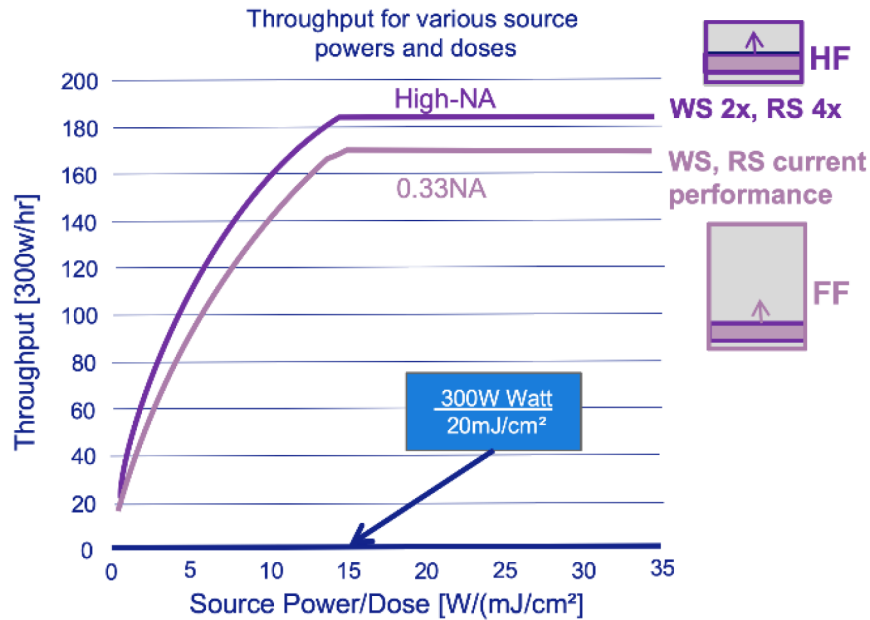


Figure 10. Throughput curves for the NXE:3400C and the high-NA system.

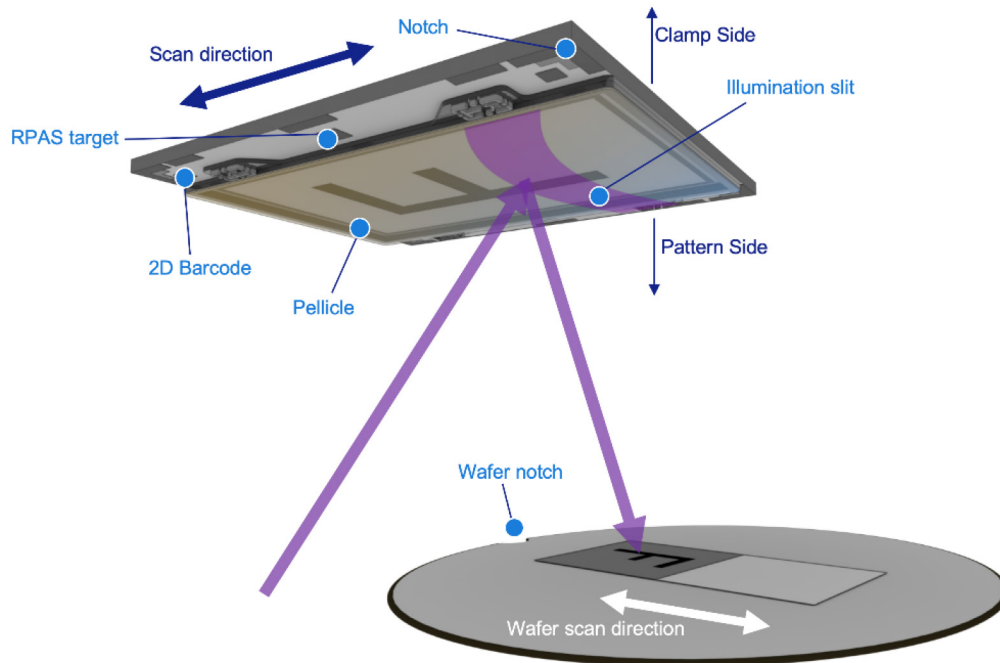


Figure 11. Definitions of the situation around the mask, main orientations of mask and wafer during printing on a 0.55NA scanner.

features to evaluate the resist: 13nm LS and 40nm staggered pillars. The first images and results are shown in figure 15.

For comparison, these results are plotted together with the 16nm LS data (figure 16). Since the resolution is present in equation 2 as a third power, the Z-factor will respond accordingly, showing an offset between the different use cases. More importantly, however, is that the descending trend continues.

6. Industrialization

Recently, a lot of progress has been shown on the manufacturing of the optics at Zeiss. Mirror metrology is in place and the first interferograms of the newly manufactured mirrors have been presented^[18]. In this paper, the status at ASML side is shown for some key components of the scan-

ner: the stages and the on-board optics interferometer system ILIAS^[21]. Next to this, the cleanrooms to assemble the high-NA scanner are being constructed.

To be able to measure the wave front of the high-NA projection optics, the ILIAS sensor has to be redesigned. The two main drivers are: the larger angles, due to the higher NA, and the improved accuracy required. A first proto sensor has been built into an existing 0.33NA scanner, and the initial results are given in figure 17.

Furthermore, a lot of progress is being made on the development of critical components, like the wafer and mask stage (figures 18 and 18).

Dedicated manufacturing equipment is also needed to mill the large frames of the EXE:5000. In figure 20 a milling machine as installed at one of our suppliers is shown. The first demonstrators are manufactured

Table 1. Mask changes and similarities 0.55NA vs 0.33NA EUV systems.

Unchanged	Changed
<ul style="list-style-type: none"> Mask blank (multilayer, absorber, capping layer, substrate) Image field size at mask level (104 x 132 mm) Exposure wavelength Mask metrology Chief Ray Angle (6°) Pellicle, pellicle infra- structure, pellicle relevant mask layout EUV pod Mask backside coating 	<ul style="list-style-type: none"> 4x/-8y magnification (the image at the wafer is flipped in y compared to the mask image) Exposure Chief Ray Angle (~5.3°) Mask frame layout <ul style="list-style-type: none"> TIS quiet zone dimension in y 45, 135° TIS (Transmission Image Sensor) RBA (Reticle Blue Align) gratings obsolete & removed Image black border size in x-direction because of larger NA in x at the mask

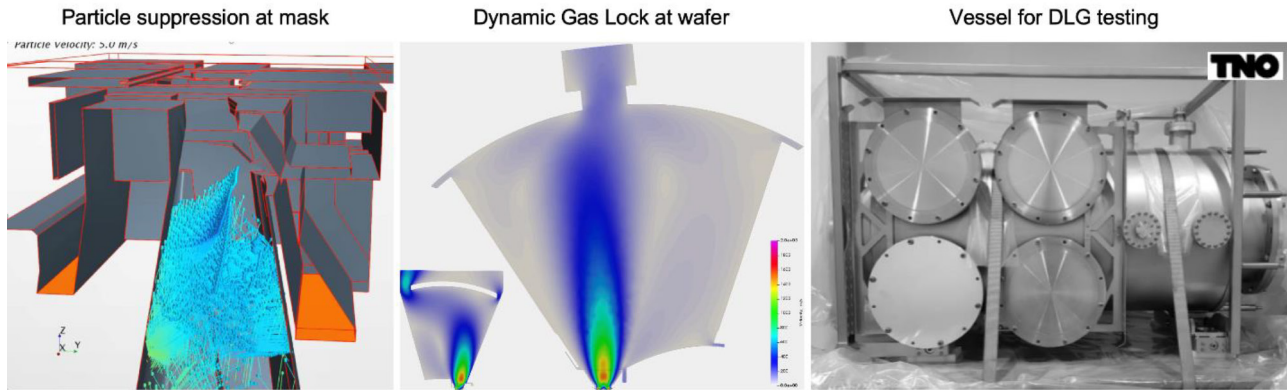


Figure 12. Particle suppression simulations at the mask (left); Equivalent Molecular Suppression simulations at the wafer; (center); Vessel for experimental validation of the molecular suppression (right).

to exhibit the capabilities of these tools.

For the final assembly, cleanrooms are being built at various locations. Note that the large reaction forces of the tool require dedicated foundation in order to ensure a sufficiently stiff fab floor, see figure 21.

7. Conclusions

In order to extend Moore's law, while controlling the stochastics to feasible levels, three parameters are key: aerial image contrast, photoresist and dose. In this paper it is shown that the high-NA system delivers the increased contrast. In combination with changes in the mask absorber, the contrast can be maintained while shrinking the resolutions. The large transmission and faster stages ensure that even at larger doses the productivity of the high-NA scanner is maintained. Key benefit of the higher NA is the obtained larger contrast. It is shown that this highly contributes to defect-free printing of eg. Contact Hole arrays.

One of the main aspects is that the main mask and pellicle properties remain unchanged. There are however some smaller differences, an overview has been outlined.

The architecture of the system is ready, as well as the main design and key components. Architectural challenges are being solved and implemented.

In order to industrialize the high-NA system, manufacturing equipment is installed all over the world. At Zeiss, optics production has started, and at ASML, the first parts for the mask and wafer stages are being built.

8. Acknowledgements

The authors would like to thank the following persons for their contributions to this paper: Jeannot Driedonkx, Jara Garcia Santaclara, Joost van Bree, Gunes Nakiboglu, Pieter de Groot, Michael Renders, Rob van Ballegoij, Claire van Lare, Frank Timmermans, Rik Hoefnagels, Lidia van

Lent, Jayson Stewart, Zuhail Tasdemir (PSI), Patrick Naulleau (CXRO), Chris Anderson (CXRO) and the High-NA teams in Wilton, San Diego, Oberkochen, and Veldhoven.

This work was partially funded by the European Commission and the Federal Ministry of Education and Research (Germany) by the EC-SEL JU Grant Agreement SeNaTe (662338, FKz 16ESE0036K), TAKE5 (692522, FKz 16ESE0072K), TakeMi5 (737479), and TAPES3 (783247, FKz 16ESE0287K).

9. References

- [1] R. Peeters, S. Lok, J. Mallman, M. van Noordenburg, N. Harned, P. Kuerz, M. Lowisch, E. van Setten, G. Schiffelers, A. Pirati, J. Stoeldraijer, D. Brandt, N. Farrar, I. Fomenkov, H. Boom, H. Meiling, and R. Kool, "EUV lithography: NXE platform performance overview," *Proc. SPIE* **9048**, (2014).
- [2] R. Schuurhuis, M. Mastenbroek, P. Jonkers, F. Bornebroek, R. Moors, K. van der Heijden, G. Fisser, P. Tayebati, and R. van Es, "0.33 NA EUV systems for HVM," *Proc. SPIE* **11323**, (2020).
- [3] J. van Schoot, E. van Setten, G. Rispens, K. Z. Troost, B. Kneer, S. Migura, J. T. Neumann, and W. Kaiser, *J. of Micro/Nanolithography, MEMS, and MOEMS*, **16**(4), 041010 (2017).
- [4] B. Geh, "EUVL: the natural evolution of optical microlithography," *Proc. SPIE* **10957**, Extreme Ultraviolet (EUV) Lithography X, 1095705 (2019).
- [5] J. G. Santaclara, B. Geh, A. Yen, T. A. Brunner, D. de Simone, J. Severi, and G. Rispens, "One metric to rule them all: new k4 definition for photoresist characterization," *Proc. SPIE* **11323**, (2020).
- [6] Joost van Bree, Private communication.

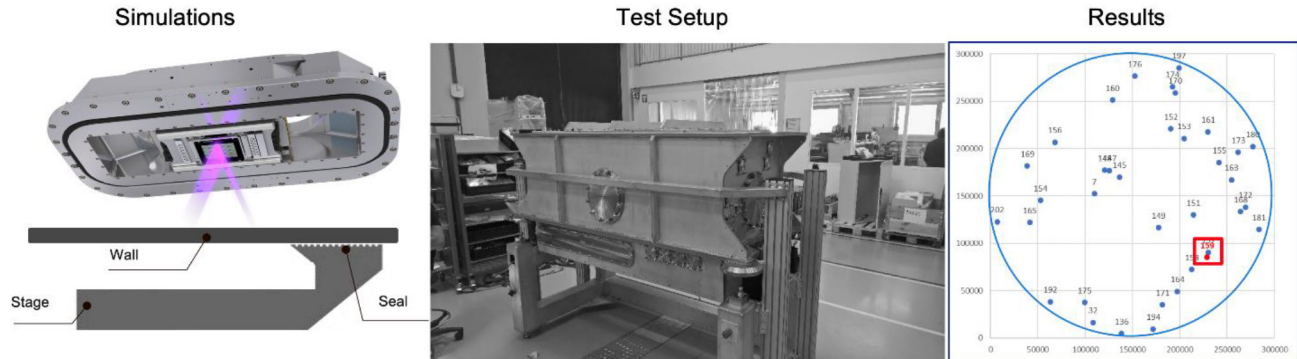


Figure 13. Avoidance of particles from cable slab in vacuum, First test results show 1 PTFE (the electrically isolating compound used in the cabled slab) particle after 46hr of operation.

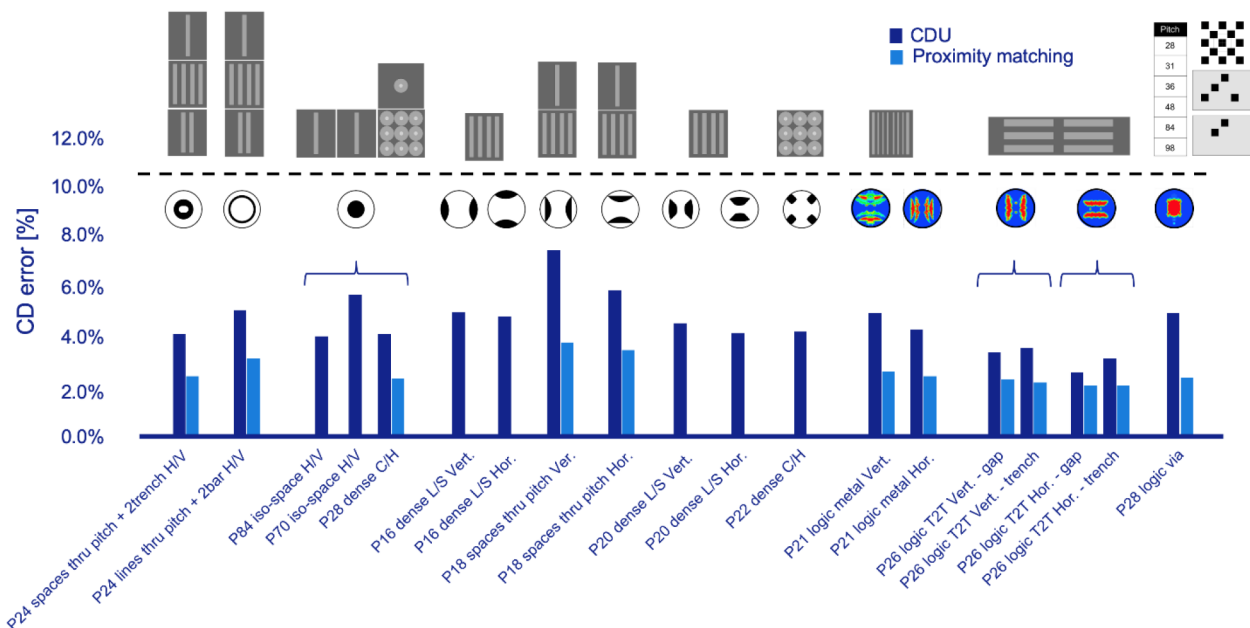


Figure 14. Overview of the critical use cases used to predict the performance of the high-NA scanner. Target specification is set at 10% of the CD of the feature. All simulations done for Ta Mask.

- [7] G. Lorusso, T. Sutani, V. Rutigliani, F. van Roey, A. Moussa, A. Charley, C. Mack, P. Naulleau, V. Constantoudis, M. Ikota, T. Ishimoto, and S. Koshihara, "The Need for LWR Metrology Standardization: The imec Roughness Protocol," **Proc. SPIE 10585**, (2018).
- [8] Jan van Schoot, Eelco van Setten, Ruben Maas, Kars Troost, Jo Finders, Sjoerd Lok, Rudy Peeters, Judon Stoeldraijer, Jos Benschop, Paul Graepner, Peter Kuerz, and Winfried Kaiser, "High-NA EUV Lithography Exposure Tool: Advantages and Program Progress," EUVL workshop, (2020).
- [9] Anthony Yen, "Continued Scaling in Semiconductor Manufacturing with Extreme-UV Lithography," EUVL workshop, (2018).
- [10] Peter De Bisschop, "Stochastic printing failures in extreme ultraviolet lithography," *Journal of Micro/Nanolithography, MEMS MOEMS Vol. 17*, Issue 4 (2018).
- [11] M.-Claire van Lare, Frank Timmermans, and Jo Finders, "Alternative reticles for low-k1 EUV imaging," **Proc. SPIE 11147**, (2019).
- [12] Frank Timmermans *et al.*, "EUV phase shift mask requirements for imaging at low-k1," **Proc. SPIE 11518**, (2020).
- [13] Eelco van Setten *et al.*, "Multilayer optimization for high-NA EUV mask3D suppression," **Proc. SPIE 11517**, (2020).
- [14] A. Pirati, J. van Schoot, K. Troost, R. van Ballegoij, P. Krabbendam, J. Stoeldraijer, E. Loopstra, J. Benschop, J. Finders, H. Meiling, E. van Setten, N. Mika, J. Dredonx, E. Stamm, B. Kneer, B. Thuring, W. Kaiser, T. Heil, and S. Migura, "The future of EUV lithography: enabling Moore's Law in the next decade" **Proc. SPIE 10143**, (2017).
- [15] J.B.P. van Schoot, C. Valentin, K. van Ingen-Schenau, and S. Migura, "EUVL lithography scanner for sub 9nm resolution," International Symposium on Extreme Ultraviolet Lithography, Washington D.C. (2014).
- [16] Jan van Schoot, Eelco van Setten, Kars Troost, Sjoerd Lok, Rudy Peeters, Judon Stoeldraijer, Jos Benschop, Joerg Zimmermann, Paul Graepner, Peter Kuerz, and Winfried Kaiser, "High-NA EUV Lithography Exposure Tool: Program Progress," **Proc. SPIE 11323**, (2020).
- [17] M. Mastenbroek, "Progress on 0.33 NA EUV systems for High-Volume Manufacturing", **Proc. SPIE 11147**, International Conference on Extreme Ultraviolet Lithography 2019, 1114703.
- [18] Lars Wischmeier, Paul Graepner, Peter Kuerz, Winfried Kaiser, Jan van Schoot, Jörg Mallmann, Joost de Pee, and Judon Stoeldraijer, "High-NA EUV lithography optics becomes reality," **Proc. SPIE 11323**, (2020).

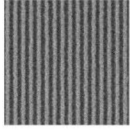
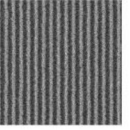
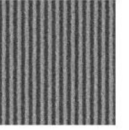
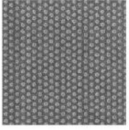
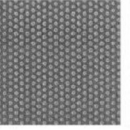
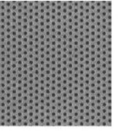
	2018	2019	2020		2018	2019	2020
Resist system¹	Non-CAR	Non-CAR	Non-CAR	Resist system¹	Non-CAR	Non-CAR	CAR
Resolution: (P26 Lines and Spaces)				Resolution: (P40 Hexagonal Pillars/CH)			
Dose [mJ/cm ²]	57	45	39	Dose [mJ/cm ²]	66	65	53
LWR _{unb} [nm]	3.1	3.0	2.9	LCDU [nm]	2.7	2.2	2.1
Z-factor [10⁻⁹mJ nm³]	1.2	0.9	0.7	Z-factor [10⁻⁹mJ nm³]	3.8	2.5	1.9

Figure 15. Continuous resist improvement for Lines/Spaces and Pillars.

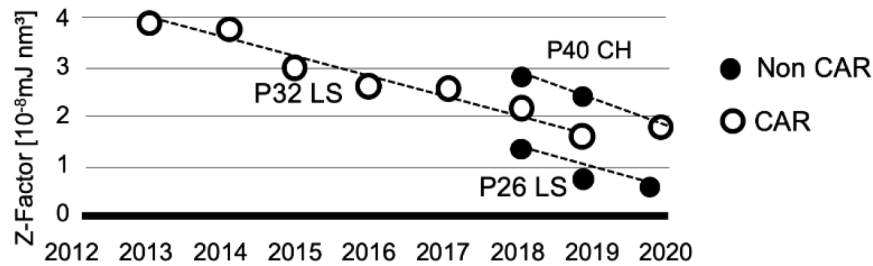
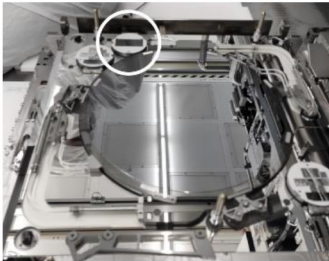
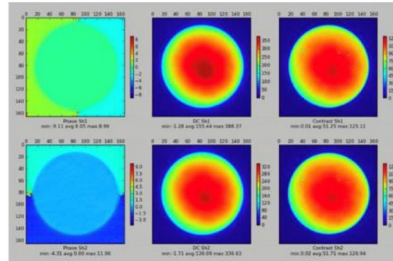


Figure 16. Continuous resist improvement for multiple use cases.

ILIAS proto sensor in NXE:3400



First camera images



First aberration results (NXE:3400)

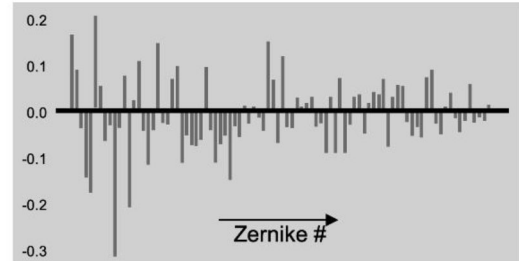
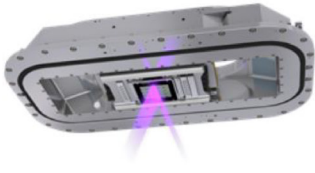


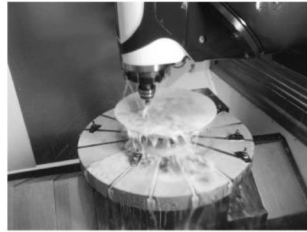
Figure 17. First images taken with high-NA ILIAS proto sensor built into NXE:3400.

- [19] Laurens de Winter, Timur Tudorovskiy, Jan van Schoot, Kars Troost, Erwin Stinstra, Stephen Hsu, Toralf Gruner, Juergen Mueller, Ruediger Mack, Bartosz Bilski, Joerg Zimmermann, and Paul Graeupner, "High NA EUV scanner: obscuration and wave front description," **Proc. SPIE 11517**, (2020).
- [20] Jan van Schoot, Koen van Ingen Schenau, Chris Valentin, and Sascha Migura, "EUV lithography scanner for sub 8 nm resolution," **Proc. SPIE 9422**, (2015).
- [21] Jan van Schoot and Hans Jasper, "Chapter 9: Fundamentals of EUVL Scanners," EUVL Lithography, ed. Vivek Bakshi, Second Edition, SPIE, (2018).

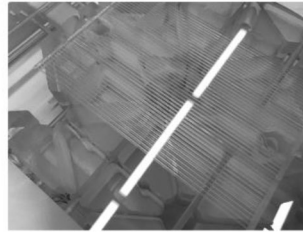
Reticle Stage design ready



Manufacturing of cooling channels



Cooling channels



First Reticle Stage short stroke

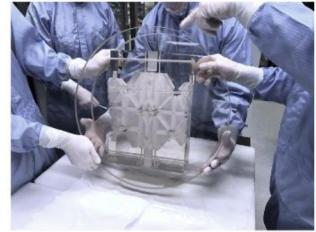
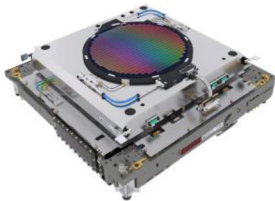
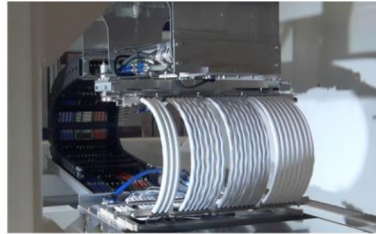


Figure 18. Progress on the mask stage short stroke module manufacturing.

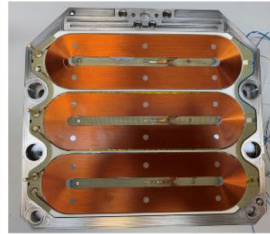
Wafer stage design ready



Cable slab dynamical testing



Proto Actuator Coils



Mirror block manufacturing started

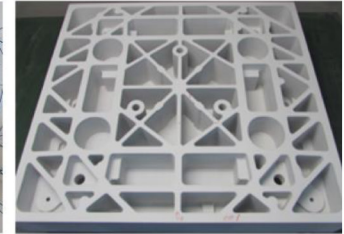
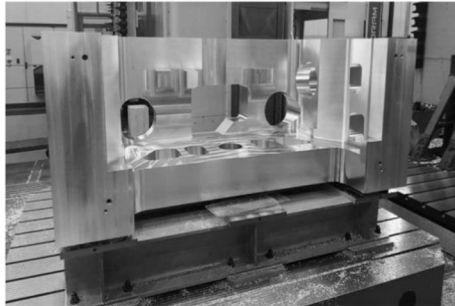


Figure 19. Wafer stage modules being manufactured.

System for final machining



Machined part of bottom frame



Rough machining of top frame



Figure 20. EXE:5000 Machining equipment for large frames.

5x5m pillars for foundation



Cleanrooms being finalized in Veldhoven, NL



New clean rooms in Wilton CT



Figure 21. High-NA cleanroom: constructions in progress.



N • E • W • S

Sponsorship Opportunities

Sign up now for the best sponsorship opportunities

Photomask Technology + EUV Lithography 2021

Contact: Melissa Valum
Tel: +1 360 685 5596; melissav@spie.org

Advanced Lithography 2021

Contact: Teresa Roles-Meier
Tel: +1 360 685 5445; teresar@spie.org

Advertise in the BACUS News!

The BACUS Newsletter is the premier publication serving the photomask industry. For information on how to advertise, contact:

Melissa Valum
Tel: +1 360 685 5596
melissav@spie.org

BACUS Corporate Members

Acuphase Inc.
American Coating Technologies LLC
AMETEK Precitech, Inc.
Berliner Glas KGaA Herbert Kubatz GmbH & Co.
FUJIFILM Electronic Materials U.S.A., Inc.
Gudeng Precision Industrial Co., Ltd.
Halocarbon Products
HamaTech APE GmbH & Co. KG
Hitachi High Technologies America, Inc.
JEOL USA Inc.
Mentor Graphics Corp.
Molecular Imprints, Inc.
Panavision Federal Systems, LLC
Profilocolore Srl
Raytheon ELCAN Optical Technologies
XYALIS

Industry Briefs

■ Taiwan Mask Poised to Raise Prices in 2Q21

<https://www.digitimes.com/news/a20210420PD210.html>

■ China Cuts Taxes to Spur Semiconductor Development

<https://www.usnews.com/news/business/articles/2021-03-29/china-cuts-taxes-to-spur-semiconductor-development>

■ White House to Hold Another Semiconductor Summit with Industry Leaders as Chip Shortage Worsens

<https://www.washingtonpost.com/technology/2021/04/09/white-house-semiconductor-shortage-chips-autos/>

■ News From the Front on Semiconductors: The Shortage Is Getting Worse.

<https://www.barrons.com/articles/news-from-the-front-on-semiconductors-the-shortage-is-getting-worse-51618613130>

■ Global Semiconductor Sales Up 14.7% Year-to-Year in February

<https://www.semiconductors.org/global-semiconductor-sales-up-14-7-year-to-year-in-february/>

■ How a Chip Shortage Snarled Everything From Phones to Cars

<https://www.bloomberg.com/graphics/2021-semiconductors-chips-shortage/>

■ Chip Shortage Will Last Beyond 2022 as Demand far Outstrips Supply, Intel Chief Says

<https://www.washingtonpost.com/technology/2021/04/13/intel-ceo-semiconductor-chip-shortage/>

Join the premier professional organization for mask makers and mask users!

About the BACUS Group

Founded in 1980 by a group of chrome blank users wanting a single voice to interact with suppliers, BACUS has grown to become the largest and most widely known forum for the exchange of technical information of interest to photomask and reticle makers. BACUS joined SPIE in January of 1991 to expand the exchange of information with mask makers around the world.

The group sponsors an informative monthly meeting and newsletter, BACUS News. The BACUS annual Photomask Technology Symposium covers photomask technology, photomask processes, lithography, materials and resists, phase shift masks, inspection and repair, metrology, and quality and manufacturing management.

Individual Membership Benefits include:

- Subscription to BACUS News (monthly)
- Eligibility to hold office on BACUS Steering Committee

spie.org/bacushome

Corporate Membership Benefits include:

- 3-10 Voting Members in the SPIE General Membership, depending on tier level
- Subscription to BACUS News (monthly)
- One online SPIE Journal Subscription
- Listed as a Corporate Member in the BACUS Monthly Newsletter

spie.org/bacushome

C A L E N D A R

2021

✱ The 36th European Mask and Lithography Conference, EMLC 2021

22 June 2021

Digital Event

www.emlc-conference.com/en

✱ SPIE Photomask Technology + EUV Lithography

26-30 September 2021

<https://spie.org/conferences-and-exhibitions/puv>

SPIE is the international society for optics and photonics, an educational not-for-profit organization founded in 1955 to advance light-based science and technology. The Society serves more than 255,000 constituents from 183 countries, offering conferences and their published proceedings, continuing education, books, journals, and the SPIE Digital Library in support of interdisciplinary information exchange, professional networking, and patent precedent. In 2019, SPIE provided more than \$5 million in community support including scholarships and awards, outreach and advocacy programs, travel grants, public policy, and educational resources. spie.org

SPIE.

International Headquarters
P.O. Box 10, Bellingham, WA 98227-0010 USA
Tel: +1 360 676 3290
Fax: +1 360 647 1445
help@spie.org • spie.org

Shipping Address
1000 20th St., Bellingham, WA 98225-6705 USA

Managed by SPIE Europe

2 Alexandra Gate, Ffordd Pengam, Cardiff,
CF24 2SA, UK
Tel: +44 29 2089 4747
Fax: +44 29 2089 4750
spieeurope@spieeurope.org • spieeurope.org

You are invited to submit events of interest for this calendar. Please send to lindad@spie.org.